



POLİTEKNİK DERGİSİ

*JOURNAL of POLYTECHNIC*

ISSN: 1302-0900 (PRINT), ISSN: 2147-9429 (ONLINE)

URL: <http://dergipark.org.tr/politeknik>



# Statistical modelling of process variables in the electrospinning production of PAN-based nanofibers

## *PAN bazlı nanofiberlerin elektroęirme ile üretiminde proses deęişkenlerinin istatistiksel modellenmesi*

*Yazar(lar) (Author(s)): Ebubekir Siddik AYDIN<sup>1</sup>, Ibrahim KORKUT<sup>2</sup>*

*ORCID<sup>1</sup>: 0000-0002-8704-4502*

*ORCID<sup>2</sup>: 0000-0002-2720-0796*

**To cite to this article:** Aydin E.S., Korkut I., “Statistical modelling of process variables in the electrospinning production of PAN-based nanofibers”, *Journal of Polytechnic*, 27(3): 1089-1099, (2024).

**Bu makaleye řu řekilde atıfta bulunabilirsiniz:** Aydin E.S., Korkut I., “Statistical modelling of process variables in the electrospinning production of PAN-based nanofibers”, *Politeknik Dergisi*, 27(3): 1089-1099, (2024).

**Eriřim linki (To link to this article):** <http://dergipark.org.tr/politeknik/archive>

**DOI:** 10.2339/politeknik.1247175

# Statistical Modelling of Process Variables in the Electrospinning Production of PAN-Based Nanofibers

## Highlight

- ❖ PAN-based nanofibers were produced via the electrospinning method
- ❖ SEM images of samples were analysed by the image processing method
- ❖ The fiber diameter was measured between 366.5 and 484.5 nm.

## Graphical Abstract

This study researches the effect of the electrospinning operation conditions on the physical properties of PAN-based nanofibers.

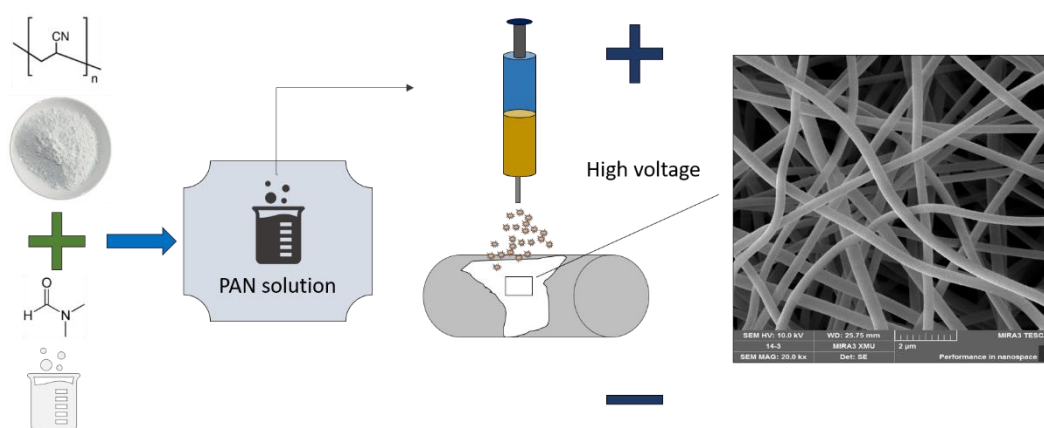


**Figure.** Experimental set-up of electrospinning of nanofibers.

## Aim

In this study, the effects of electrospinning operating parameters on the physical properties of nanofibers were investigated.

## Design & Methodology

SEM images of the nanofibers produced with the experimental plan created with the central composite design were processed and the diameter and porosity values were revealed.

## Originality

The effects of electrospinning operating parameters such as flow rate, voltage and distance to the collector on the diameter, porosity and water absorption capacity of nanofibers were investigated statistically and findings on the experimental control of fiber structures were provided.

## Findings

As a result of the analysis of 17 experiments performed according to the experimental plan, the fiber diameter range was found to be 366.5-484.5 nm, the porosity value was 0.333-0.446, and the water absorption capacity was between 868%-5712%.

## Conclusion

The most important variable affecting fiber diameter is the distance to the collector, in addition, voltage, and flow rate also have moderate effects.

## Declaration of Ethical Standards

The authors of this article declare that the materials and methods used in this study do not require ethical committee permission and/or legal-special permission.

# Statistical Modelling of Process Variables in the Electrospinning Production of PAN-Based Nanofibers

*Araştırma Makalesi / Research Article*

**Ebubekir Siddik AYDIN<sup>1\*</sup>, Ibrahim KORKUT<sup>1</sup>**

<sup>1</sup>Sivas University of Science and Technology, Department of Chemical Engineering, 58000, Sivas, Turkey  
(Geliş/Received : 03.02.2023 ; Kabul/Accepted : 08.03.2023 ; Erken Görünüm/Early View : 02.04.2023)

## ABSTRACT

In this study, the effects of the electrospinning operating parameters such as flow rate (1-5 ml/h), voltage (15-30 kV), and distance to the collector (100-200 mm) on the physical properties of PAN-based nanofibers were investigated statistically by applying the central composite design method. The minimum nanofiber diameter was found to be 366.5 nm, under operating conditions of 5 ml/h flow rate, 30 kV, and 100 mm distance to the collector. Experimental conditions of 15 kV, 5 ml/h flow rate, and a 200 mm distance to the collector, a maximum porosity value of 0.446 was obtained. Similarly to the porosity, the water absorption capacity (WAC) value did not show a linear increase, and the maximum absorption capacity was calculated as 5712%, and at that point where the diameter is relatively large and the porosity is low.

**Keywords:** PAN, electrospinning, fiber diameter, porosity, water absorption capacity.

## PAN Bazlı Nanofiberlerin Elektroğirme ile Üretiminde Proses Değişkenlerinin İstatistiksel Modellenmesi

### ÖZ

Bu çalışmada, akış hızı (1-5 ml/sa), voltaj (15-30 kV) ve kolektöre olan mesafe (100-200 mm) gibi elektroğirme çalışma parametrelerinin PAN bazlı nanofiberlerin fiziksel özelliklerine etkisi, merkezi kompozit tasarım yöntemi uygulanarak, istatistiksel olarak incelenmiştir. 5 ml/sa akış hızında, 30 kV voltajda ve kolektöre 100 mm mesafedeki çalışma koşullarında minimum nanofiber çapı 366,5 nm olarak bulunmuştur. 15 kV, 5 ml/sa akış hızı ve kolektöre 200 mm mesafe uzaklıktaki deney koşullarında, maksimum gözeneklilik değeri 0,446 olarak elde edilmiştir. Gözenekliliğe benzer şekilde, su tutma kapasitesi (STK) değeri doğrusal bir artış göstermemiş ve maksimum absorpsiyon kapasitesi %5712 olarak hesaplanmış ve bu noktada çapın nispeten büyük ve gözenekliliğin düşük olduğu nokta olarak belirlenmiştir.

**Anahtar kelimeler:** PAN, elektroğirme, fiber çapı, gözeneklilik, su tutma kapasitesi.

### 1. INTRODUCTION

Today, carbon fibers are important materials used in many applications due to their high surface areas, lightness, low density, high tensile strength, and excellent chemical resistance [1–3]. Moreover, it has found applications in many areas such as aviation, automobile industry, wastewater treatment [4, 5], energy applications [6, 7], and wearable handmade wound dressings [8]. According to some reports, the demand for carbon fibers will reach 120,000 tons in 2022 in parallel with the increasing application areas [9]. In addition, the use of polymer-based carbon fiber in composite structures increases this demand [10, 11].

One of the methods of producing carbon fiber is electrospinning, which spins a polymer solution into fine fibers in an electrical field. By the electrospinning method, different types of polymers can be formed with controllable morphology and diameter [12, 13].

\*Sorumlu Yazar (Corresponding Author)  
e-posta : esaydin@sivas.edu.tr

Electrospinning for polymer-based carbon fiber production is simple (less process steps) and inexpensive, making it a cost-effective option for large-scale production than conventional methods such as wet spinning. In addition, among these polymers, Polyacrylonitrile (PAN) is a widely used precursor material in the production of carbon nanofibers (CNFs) and has good stability and mechanical properties [14]. As a result of this process, fibers are also very uniform in size and shape, which is an important feature for a variety of applications. A versatile material with many potential applications from aerospace to sports equipment, carbon fibers' properties such as stiffness, thermal stability, and mechanical strength are determined by their diameter [15]. The diameter of the carbon fiber refers to the thickness of each fiber and plays a crucial role in determining the properties and suitability of the fiber for different applications. While relatively small diameter fibers have higher strength and stiffness, this makes them more suitable for high performance applications such as aerospace and automotive. Larger diameter carbon fibers are easier to process because they are more flexible,

making them more suitable for areas such as textiles and composites [16]. Demonstrating the relationship between carbon fiber diameter and properties is crucial to selecting the appropriate fiber for specific applications. Another factor affecting the performance of carbon fibers in various applications is porosity. Porosity refers to the presence of voids or empty spaces within a material. Porosity measurement in carbon fibers can be determined by various methods, such as helium pycnometry (HP), mercury intrusion porosimetry (MIP), or nitrogen adsorption [17, 18]. In addition to this, studies on determining porosity by image processing method from obtained Scanning electron microscopy (SEM) images are also encountered in the literature [19]. The porosity of carbon fibers can vary depending on the method used. For example, nitrogen adsorption is used to measure the micro-porosity of carbon fibers, while MIP is typically used to measure the macro-porosity of carbon fibers. The results obtained from SEM analyses cannot express the macro and micro pore structure of the material and it is essential to get an easy and fast method to evaluate the surface structure. In addition to the above information, the carbon fibers are used in many water filter media such as reverse osmosis, and ultrafiltration filters. However, it is very important to determine the water absorption capacity of the fiber and to make the appropriate fiber application match correctly. In the literature, Response surface methodology (RSM) studies have been carried out for the optimization of the properties of nanofibers obtained from polymers by electrospinning method [20–22]. In this study, the central composite design-RSM methodology was used to optimize the physical properties of the PAN precursor fibers produced by electrospinning. For this purpose, the effects of three main electrospinning processing parameters (flow rate, voltage, and distance-to-collector) on the diameter, porosity, and water absorption capacity of electrospun PAN were investigated.

## 2. MATERIALS AND METHOD

N,N-Dimethylformamide (DMF) Reagent Plus® (Cas No: 68-12-2), and Polyacrylonitrile (average molecular weight,  $M_w$ : 150 000) were purchased from Sigma Aldrich and used as received. To prepare the polymer solution, 54 g of DMF was weighed and taken into a jar. Then, a PAN solution containing 10% by weight was prepared by adding 6 g of PAN to the DMF solution. A homogeneous appearance was obtained by mixing the prepared solution in a magnetic stirrer at 300 rpm for 24 hours in a closed medium. In order to remove the air bubbles in the solution, the PAN solution was kept for another 24 hours. Fytronix ES-9000 electrospinning device was used for the electrospinning process with adjustable drum speed, pump flow rate, voltage, and distance-to-collector. The experimental setup of PAN electrospinning experiments is presented in Fig 1.

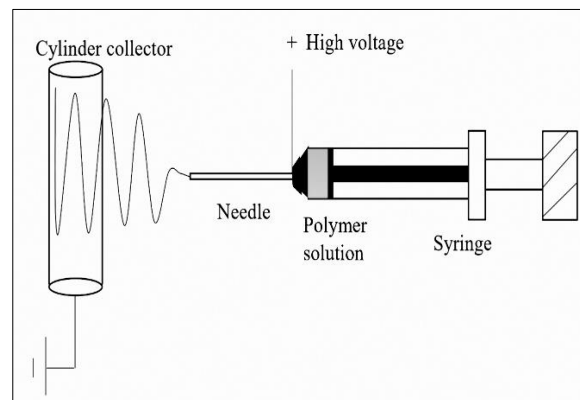


**Figure 1.** Schematic of experimental setup

A plastic syringe with a volume of 20 ml, with a 22g stainless steel needle, was used in all experiments. The drum speed was kept constant at 250 rpm. Before electrospinning, collector drum was covered with 12  $\mu$ m thick aluminium foil. Ensuring the obtained nanofibers were sufficient for SEM analysis, each electrospinning was continued for 1 hour. The nanofibers obtained after electrospinning were mechanically separated from the aluminium foil. The separated nanofibers were stabilized by keeping them in an atmospheric environment at 200 °C for 1 day. SEM analysis was carried out by using a TESCAN MIRA3 XMU high-resolution field emission scanning electron microscope for measuring nanofiber diameters. Prior to SEM analysis, a thin gold layer was sputtered on each sample by using a Quorum Technologies Q150T sputter coater to avoid charging.

### 2.1. Determination of Experimental Conditions

There are many widespread applications of “Response Surface Methodology” in the fields of optimization, model development, and variable screening. For this reason, a response surface methodology central composited design (face-centered, full,  $\alpha=1$ ) was studied. The variables used in creating the model and their low and high-level factors are given in Table 1. The CCD design experimental plan consisted of 17 experiments, assigning 14 non-center points and 3 additional center points. In the statistical experimental plan, three numerical factors flow rate (A), voltage (B), and distance-to-collector (C) were chosen as process factors, and diameters of nanofibers, porosity, and water absorption capacity values (%) were selected as process responses R1, R2, and R3 respectively.

**Table 1.** Variables and numeric values

Factors	Low level ( $\alpha = -1$ )	High level ( $\alpha = +1$ )
Flow rate (ml/h)	1	5
Voltage (kV)	15	30
Distance (mm)	100	200

### 2.2. Determination of Fiber Diameter

In this context, in order to reveal the diameter properties of the prepared electrospun PAN fibers, the obtained SEM images were analyzed with the SIMPoly

(A Matlab-Based Image Analysis Tool) approach developed by Murphy et al. [23], and the diameter values were calculated. As a result of this approach, which was validated by a very reliable method in diameter measurement such as DiameterJ, the diameter measurements of the fibers were determined quite accurately. SEM images of Run 14, and the histogram used to determine diameter values are shown in Figure 2.

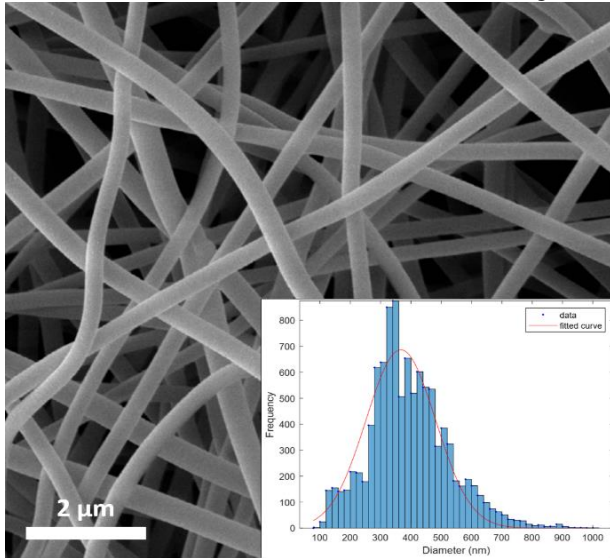


**Figure 2.** SEM image of the RUN 14 and its histogram (Experimental conditions: Flow rate=5 ml/h, Voltage=30 kV, Distance=100 mm)

### 2.3. Determination of Fiber Porosity

Porosity values were determined by processing the images of SEM analysis using MATLAB software 2022b (Math Works Co.). The SEM image, which is currently in gray scale, was converted to binary format by applying the global threshold process. After the conversion, the black pixel points got the value 0, while the white pixel points got the value 1. Pixels equal to or higher than the global threshold belongs to the fiber, while the remaining values represent part of the background. Porosity (P) is calculated using the following average image density equation; where n is the number of white pixels, and N is the total number of pixels [24]:

$$P = \left(1 - \frac{n}{N}\right) \times 100 \quad (1)$$

### 2.4. Determination of Fiber Water Absorption Capacity

A predetermined amount of each PAN-based nanofiber was immersed in distilled water. All tests were performed at a laboratory temperature of 23 °C. The samples were removed from the water at certain intervals and weighed with a precision balance (Ohaus PR224) and this process was continued until the weighing result reached a certain equilibrium point. The water absorption capacity of the samples was calculated with the following equation [25].

$$WAC = \left[\frac{W_t - W_0}{W_0}\right] \times 100 \quad (2)$$

where WAC is the water absorption capacity,  $W_0$  is the dry weight of the sample, and  $W_t$  is the wet weights of the sample.

## 3. RESULTS AND DISCUSSION

In this study, a quadratic model was chosen, which includes main factors, two-term interactions, and second-order factors. The CCD experiment plan shown in Table 2 was created using Design-Expert, trial version 13.0. Three regression methods namely, stepwise selection, forward selection, and backward elimination were separately implemented to the experimental data in the model development. Among the three regression methods, "backward elimination" gave better performance. For this purpose, the statistical indicators considered were predictive correlation coefficient ( $R^2_{pred.}$ ), and adjusted correlation coefficient ( $R^2_{adj.}$ ). A 5% confidence level was performed to detect significant terms in the model in the variance analysis (ANOVA). The model with the highest  $R^2$  value and the least difference between  $R^2_{adj.}$  and  $R^2_{pred.}$  was selected. The regression models and their statistical evaluations are presented in this section. Analysis of variance is given for nanofiber diameter, porosity, and water absorption capacity in Table 3-5, respectively. Statistical indicators of models developed for all three responses are given in Table 6, and model equations in terms of both actual and coded factors are introduced. The model terms are significant which are p-values less than 0.05. As seen in Table 3, A, B, C, AB, AC, BC,  $A^2$ ,  $B^2$  and  $C^2$  are important terms of models affecting of nanofiber diameters. A Lack of Fit F-value of 2.04 means that the Lack of Fit is not significant relative to pure error.

**Table 2.** Experimental plan, average diameter, porosity, and water absorption capacity values of nanofibers

Run	(A) Flow rate (ml/h)	(B) Voltage (kV)	(C) Distance (mm)	(R1) Fiber diameter (nm)	(R2) Porosity	(R3) WAC(%)
1	3	22.5	150	475.0	0.364	2033
2	5	22.5	150	451.8	0.366	868
3	5	30	200	445.5	0.364	1305
4	3	30	150	480.8	0.347	3133
5	5	15	100	394.2	0.419	3602
6	5	15	200	411.5	0.446	4273
7	3	15	150	443.4	0.382	3143
8	1	30	200	450.0	0.346	5712
9	1	30	100	417.3	0.397	5288
10	3	22.5	100	424.1	0.380	3059
11	3	22.5	200	447.8	0.359	2346
12	1	15	100	428.2	0.400	2116
13	1	15	200	370.2	0.333	1725
14	5	30	100	366.5	0.354	1591
15	3	22.5	150	484.5	0.350	1850
16	3	22.5	150	475.2	0.377	2057
17	1	22.5	150	472.3	0.373	1060

**Table 3.** Analysis of variance of the second-ordered model used to determine the diameters of nanofibers

Source	SS	df	MS	F-value	p-value	
<b>Model</b>	21120.80	9	2346.76	45.71	< 0.0001	significant
A-Flow rate	467.45	1	467.45	9.11	0.0195	
B-Voltage	1264.50	1	1264.50	24.63	0.0016	
C-Distance	895.29	1	895.29	17.44	0.0042	
AB	491.10	1	491.10	9.57	0.0175	
AC	1845.89	1	1845.89	35.96	0.0005	
BC	2906.27	1	2906.27	56.61	0.0001	
A <sup>2</sup>	488.37	1	488.37	9.51	0.0177	
B <sup>2</sup>	484.04	1	484.04	9.43	0.0181	
C <sup>2</sup>	4207.02	1	4207.02	81.95	< 0.0001	
<b>Residual</b>	359.36	7	51.34			
Lack of Fit	300.56	5	60.11	2.04	0.3602	not significant
Pure Error	58.80	2	29.40			
<b>Cor Total</b>	21480.16	16				

SS: sum of squares; df: degree of freedom; MS: mean square

**Table 4.** Analysis of variance of the reduced quadratic model used to determine the porosity values of nanofibers

Source	SS	df	MS	F-value	p-value	
<b>Model</b>	0.0120	6	0.0020	15.74	0.0001	significant
A-Flow rate	0.0010	1	0.0010	7.73	0.0194	
B-Voltage	0.0030	1	0.0030	23.43	0.0007	
C-Distance	0.0011	1	0.0011	8.39	0.0159	
AB	0.0031	1	0.0031	24.44	0.0006	
AC	0.0030	1	0.0030	23.58	0.0007	
A <sup>2</sup>	0.0009	1	0.0009	6.84	0.0258	
<b>Residual</b>	0.0013	10	0.0001			
Lack of Fit	0.0009	8	0.0001	0.6436	0.7309	not significant
Pure Error	0.0004	2	0.0002			
<b>Cor Total</b>	0.0133	16				

SS: sum of squares; df: degree of freedom; MS: mean square

As seen in Table 4, A, B, C, AB, AC, and A<sup>2</sup> are significant model terms of porosity values. The Lack of Fit F-value of 0.64 means the Lack of Fit is not significant relative to the pure error.

**Table 5.** Analysis of variance of the reduced quadratic model used to determine the water absorption capacity of nanofibers

Source	SS	df	MS	F-value	p-value	
<b>Model</b>	3.062E+07	7	4.374E+06	34.46	< 0.0001	significant
A-Flow rate	1.816E+06	1	1.816E+06	14.31	0.0043	
B-Voltage	4.709E+05	1	4.709E+05	3.71	0.0862	
C-Distance	8702.50	1	8702.50	0.0686	0.7993	
AB	1.842E+07	1	1.842E+07	145.09	< 0.0001	
A <sup>2</sup>	2.052E+06	1	2.052E+06	16.17	0.0030	
B <sup>2</sup>	4.519E+06	1	4.519E+06	35.61	0.0002	
C <sup>2</sup>	1.997E+06	1	1.997E+06	15.73	0.0033	
<b>Residual</b>	1.142E+06	9	1.269E+05			
Lack of Fit	1.117E+06	7	1.595E+05	12.44	0.0764	not significant
Pure Error	25638.00	2	12819.00			
<b>Cor Total</b>	3.176E+07	16				

SS: sum of squares; df: degree of freedom; MS: mean square

As seen in Table 5, A, B, C, AB, A<sup>2</sup>, B<sup>2</sup>, and C<sup>2</sup> are significant model terms of water absorption capacity.

$$\sigma_B = \sqrt{\sigma^2 + 4\tau^2} \quad (4)$$

In all three models, A, B, and C are the main terms, AB intermediate interaction term, and A<sup>2</sup> quadratic term. All three models include A, B, and C main terms, AB interaction term, and A<sup>2</sup> quadratic term. Nanofiber diameter, porosity, and water absorption capacity vary depending on flow rate, applied voltage, and distance between collector drum and syringe. B<sup>2</sup> and C<sup>2</sup> are quadratic terms of nanofiber diameter and water absorbance capacity models. Statistical indicators of the developed models are given in Table 6. The nanofiber average diameter is 437.56 nm, while R<sup>2</sup>, R<sup>2</sup><sub>adj.</sub> and R<sup>2</sup><sub>pred.</sub> values were found as 0.9833, 0.9618, and 0.8091, respectively. While the correlation coefficient value was at the highest value in the fiber diameter, it showed a slight decrease for the water absorption capacity model, and the lowest value was calculated as 0.9042 for the porosity value. R<sup>2</sup><sub>pred.</sub>, which also shows the degree of estimation of porosity value was calculated as 0.7123. In the literature, there are some different assumptions in the detection of porosity by image processing. In some papers, white pixel points were used to calculate the porosity value, but in our porosity calculation approach, black pixel points were used to calculate the porosity value (Equation 1). Here, the difference arises from the definition of the concept of porosity. In our study, the black pixel dots were chosen to represent the spaces between the fibers, and the ratio of the total number of pixels was calculated as the porosity value. Otherwise, the selection of white pixel dots refers to the total solid ratio rather than the porosity. Therefore, the porosity values we obtained were calculated relatively less than the studies in the literature.

**Table 6.** Statistical indicators of the developed models

Nanofiber diameters (R1)			
Std. Dev.	7.17	R <sup>2</sup>	0.9833
Mean	437.56	R <sup>2</sup> <sub>adj.</sub>	0.9618
C.V. %	1.64	R <sup>2</sup> <sub>pred.</sub>	0.8091
Porosity (R2)			
Std. Dev.	0.0113	R <sup>2</sup>	0.9042
Mean	0.3746	R <sup>2</sup> <sub>adj.</sub>	0.8468
C.V. %	3.01	R <sup>2</sup> <sub>pred.</sub>	0.7123
Water absorption capacity (R3)			
Std. Dev.	356.27	R <sup>2</sup>	0.9640
Mean	2656.53	R <sup>2</sup> <sub>adj.</sub>	0.9361
C.V. %	13.41	R <sup>2</sup> <sub>pred.</sub>	0.8410

After the statistical data were presented, the information about the correlations obtained for the 3 responses is given in Table 7, as were coded and real values, respectively.

**Table 7.** Model equations for the physical properties of PAN nanofiber

<b>Fiber diameter</b> = 467.72- 6.84A +11.25B +9.46C - 7.84AB+15.19AC +19.06BC -13.50A <sup>2</sup> -13.44B <sup>2</sup> -39.63C <sup>2</sup> (coded)
<b>Fiber diameter</b> = 121.51 +5.80A+6.19B +3.34C - 0.52AB +0.15AC +0.05BC -3.37A <sup>2</sup> -0.24B <sup>2</sup> -0.02C <sup>2</sup> (actual)
<b>Porosity</b> = 0.366 +0.0099A -0.0173B - 0.0103C- 0.0197AB + 0.0194AC +0.0145A <sup>2</sup> (coded)
<b>Porosity</b> = 0.465 -0.0163A+ 0.001641B-0.000788C -0.001314AB + 0.000194AC+0.003635A <sup>2</sup> (actual)
<b>WAC</b> = 1899.55 -426.20A +217.00B -29.50C - 1517.25AB -875.21A <sup>2</sup> + 1298.79B <sup>2</sup> +863.29C <sup>2</sup> (coded)
<b>WAC</b> = 12638.19 +3375.59A -706.65B -104.18C - 101.15AB - 218.80A <sup>2</sup> +23.09B <sup>2</sup> +0.34C <sup>2</sup> (actual)

Figure 3 representing the plots between the predicted data and the actual experimental data of nanofiber diameters, porosity, and water absorption capacity proves the reliability of the models. In accordance with the correlation coefficient values given in Table 6, the distribution of the predicted values with respect to the

rate. Figure 5 illustrates the effect of applied voltage on nanofiber diameter. By increasing the applied voltage from 15 kV to 30 kV, the diameter of the produced nanofibers increases. At low voltage and an average constant flow rate, the diameter of the nanofibers changes slightly with the change in distance, while at a high voltage and constant flow rate, the diameter of the nanofibers is more affected by the change in distance. In Figure 6, the effect of distance and applied voltage on the diameter of nanofibers at different flow rates were presented. While the nanofiber diameter is large at a low flow rate, the nanofiber diameter becomes smaller at a high flow speed. The diameter of the nanofibers ranges from 366.5 nm to 484.5 nm. The mean nanofiber diameter is 437.56 nm and the standard deviation value is 7.2 nm. The coefficient of variation (% C.V.) is 1.64% depending on the mean and standard deviation value. In nanofiber production, it is generally desired to minimize the diameter of the nanofibers in order to increase the surface area and mechanical properties of the obtained nanofiber. Considering the experimental results, it is necessary to apply a high flow rate, high voltage difference, and low distance between the syringe and collector drum for reducing the diameter of nanofibers. The experimental results obtained in this study were

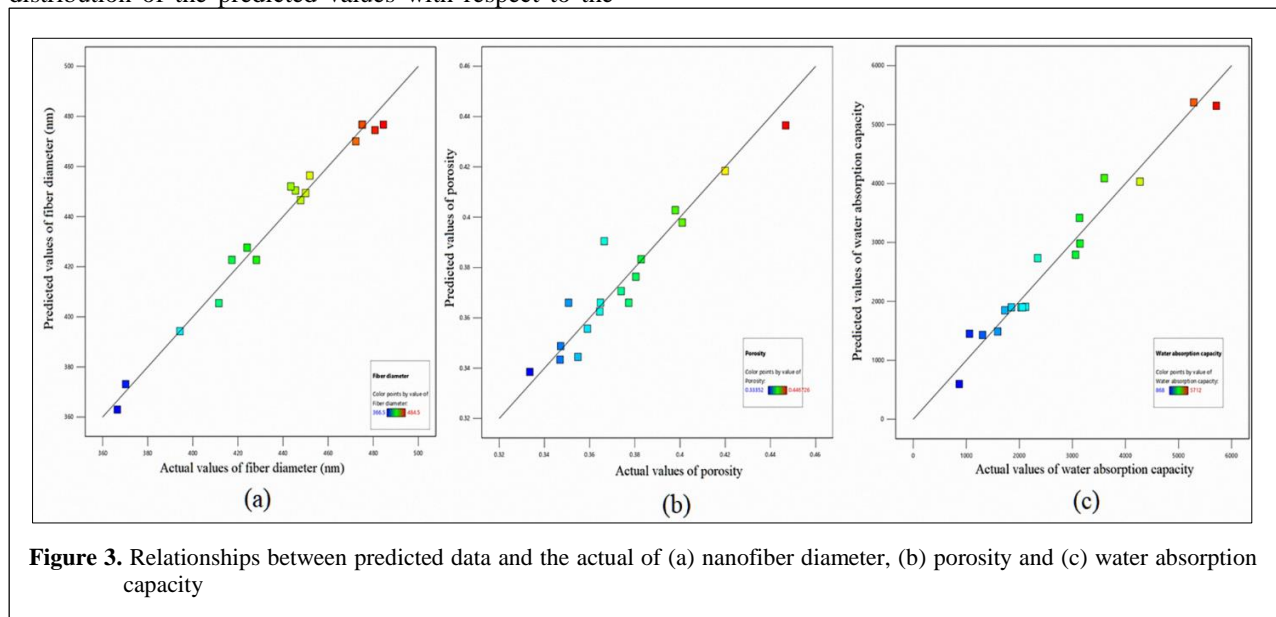


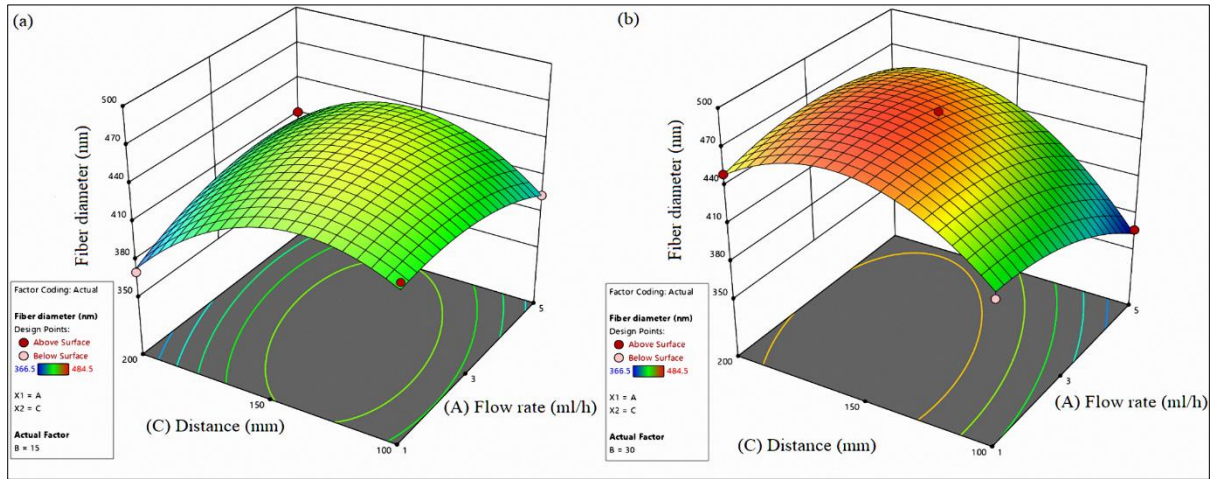
**Figure 3.** Relationships between predicted data and the actual of (a) nanofiber diameter, (b) porosity and (c) water absorption capacity

actual values is as water absorption capacity, fiber diameter, and porosity, from the highest accuracy to the lowest accuracy, respectively.

As seen in Figure 4, the diameter of the nanofibers varies when the flow rate is changed between 1-5 ml/h and the voltage is changed between 15-30 kV, and when the distance of the syringe tip to the collector is adjusted from 100 m to 200 mm. It would not be correct to talk about a linear correlation here. As seen in Figure 4a, fiber diameters decrease in transitions from medium voltage values to maximum voltage values and from low flow in 4b, when the distance is set to 200 mm, lower fiber diameter values are observed at low voltage and flow

carried out with a 10 % solution of 150,000 molecular weight PAN in DMF. The results may differ for different molecular weights of PAN samples and different concentrations of PAN solution. Porosity is generally expressed as a percentage and is calculated by dividing the volume of pores by the volume of bulk. The porosity in the obtained nanofibers is due to the remaining microporosity between the nanofibers stacked on each other. It should be considered that the porosity values derived from the results obtained from the SEM analysis





may not fully reflect the bulk structure due to the SEM image obtained from the surface but anyway, there is a robust relationship between porosity values and process factors. When Figures 7a and 7b are

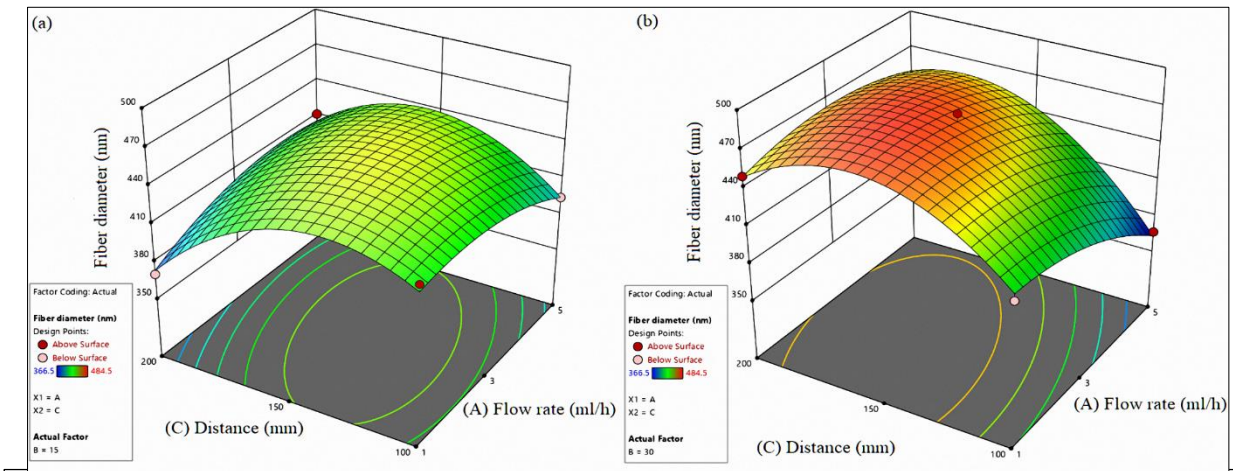


**Figure 4.** The effect of interaction between flow rate (A) and voltage (B) on diameters of nanofibers at different distances of (a) 100 mm (b) 200 mm

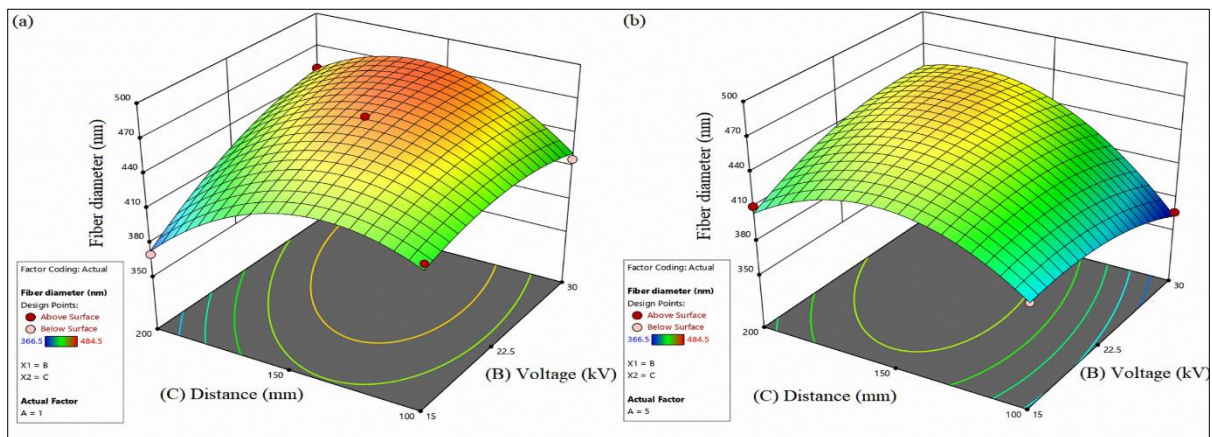


**Figure 5.** The effect of interaction between flow rate (A) and distance (C) on diameters of nanofibers at different voltages (a) 15 kV (b) 30 kV

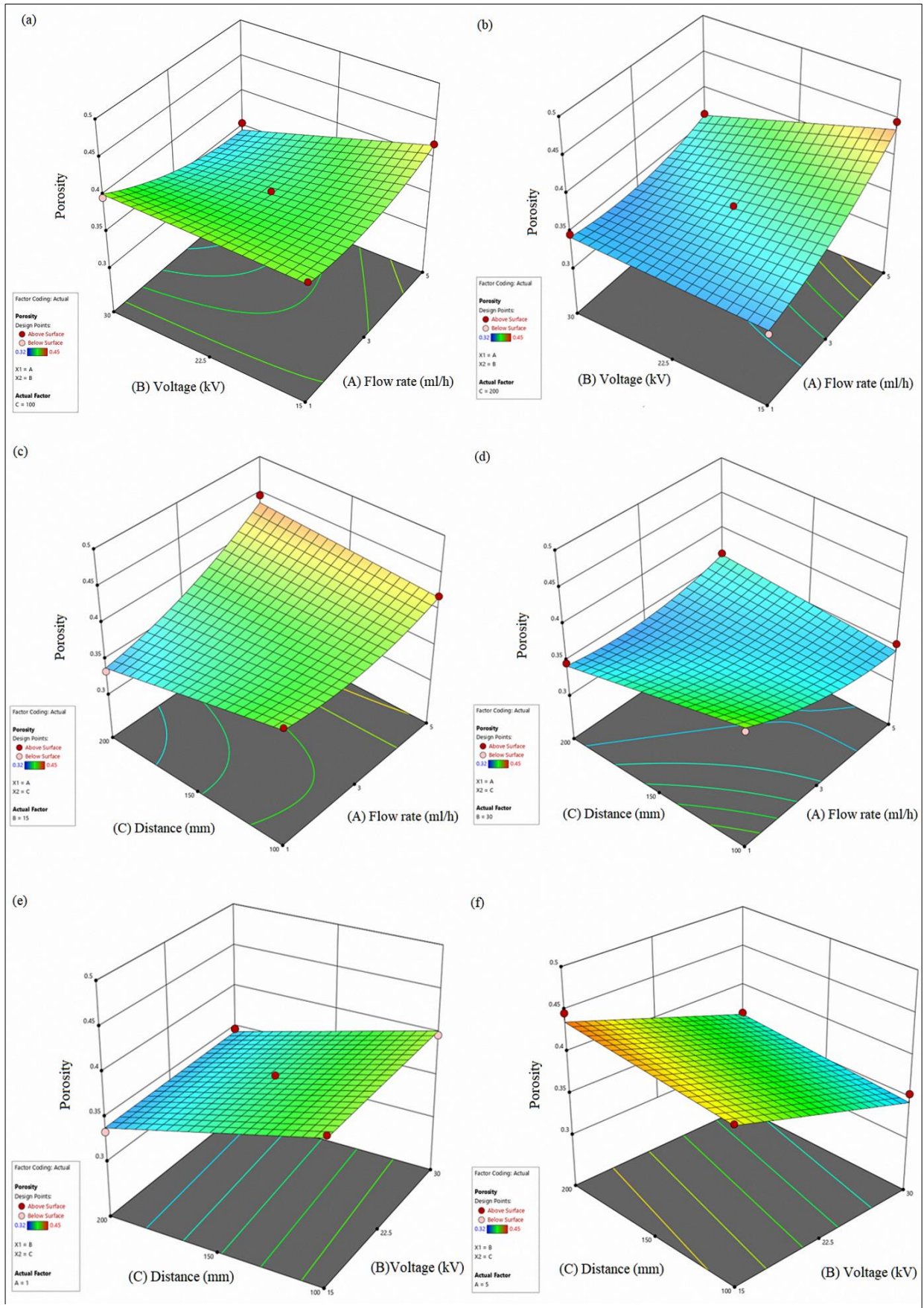
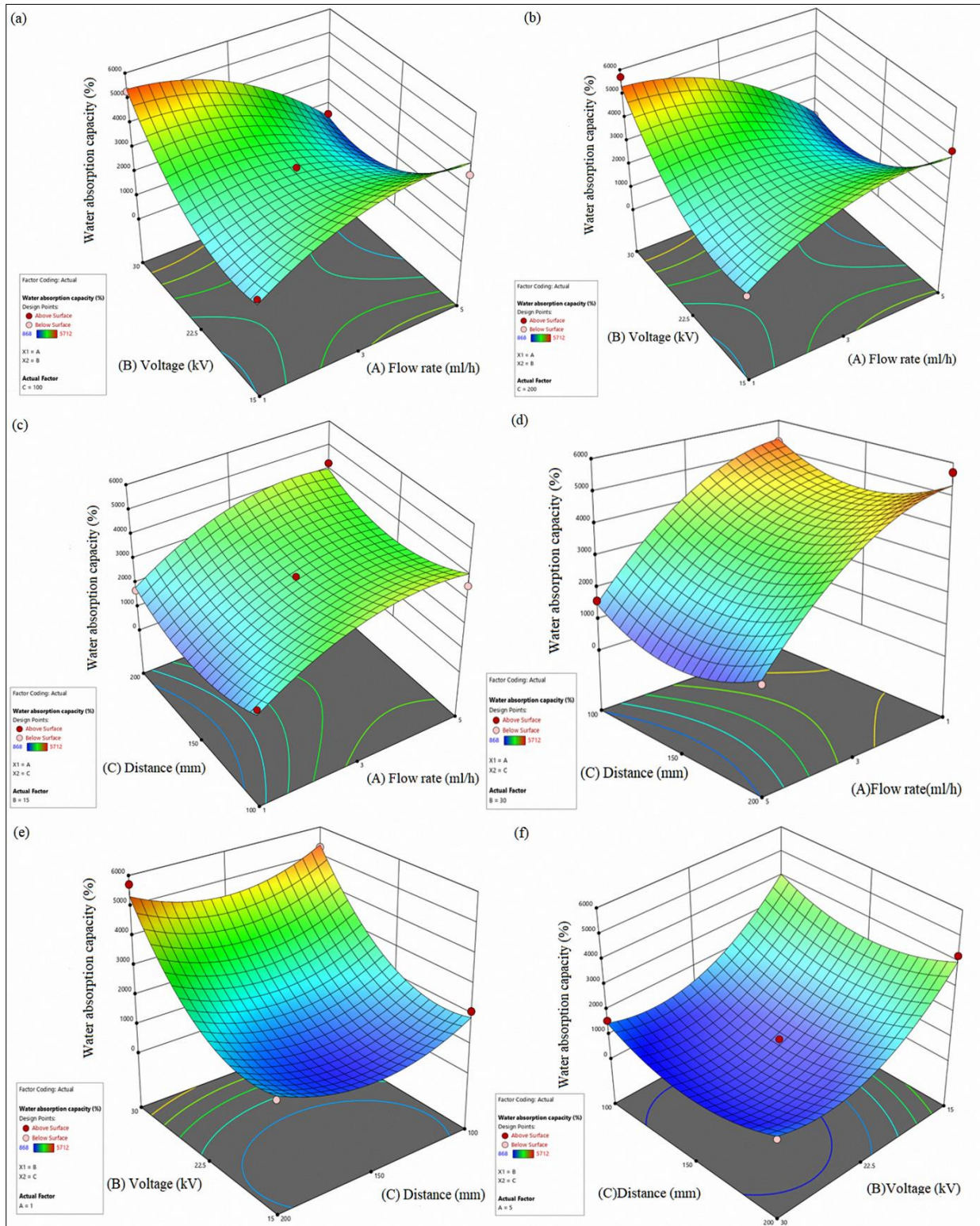


Figure 7. The effects of variables on porosity values of nanofibers



**Figure 8.** The effects of variables on the water absorption capacity

compared, it is seen that the porosity value decreases with increasing distance due to less stacking of PAN nanofibers. Similarly, as seen in Fig. 7c and 7d as the voltage increases, the PAN nanofibers will be better stacked on top of each other, and the porosity value will be reduced by a decrease in the space between PAN

nanofibers. Figure 7e and 7f show the effects of distance and voltage variables on the porosity value at different flow rate 1 ml/h and 5 ml/h, respectively. According to the results of the analysis of variance, porosity is affected by main and quadratic terms of flow rate and interactions in terms of flow rate-voltage (AB)

and flow rate-distance (AC). Therefore, when the flow rate is changed for controlling the porosity, other variables need to be carefully adjusted. Absorption is a physical process that incorporation of any substance into different forms of another substance (for instance, gases can be absorbed by liquids, or liquids can be absorbed by solids). The absorption capacity of a material is determined by its ability to absorb water when immersed in it. According to the definition of water absorption capacity, the weight of water absorbed by a material in the saturated state is compared to the weight of the dry material, and it varies depending on the material's properties, especially its porosity, surface and bulk properties. WAC of the produced PAN nanofibers was determined after determining and modelling their diameter and porosity, and a relationship was explained between WAC and the electrospinning variables. It has been shown that PAN's water absorption capacity has affected all three main factors, flow rate-voltage interaction term (AB) as well as all quadratic terms of factors ( $A^2$ ,  $B^2$ , and  $C^2$ ). Due to differences in experimental conditions, water absorption capacity varies from 868% to 5712%. Absorbent materials may have different levels of capacity based on their final application or requirement. A decrease in water absorption capacity is observed at low flow rates, as shown in Figures 9a and 9b. In response to an increase in voltage, the capacity to absorb water increases although the flow rate was increased. Since the water absorption capacity depends on the porosity and the physical properties of the material, it is seen that the voltage and flow rate, which are the effective variables of the porosity and also affect the water absorption capacity.

#### 4. CONCLUSION

An experimental study was carried out to investigate the effects of electrospinning operating parameters on the physical properties of PAN-based fibers and the results were statistically interpreted. The outputs obtained as a result of the study can be summarized as follows:

✓ The most important variable which affecting the fiber diameter is the distance to the collector, but there are also moderate effects of voltage and flow rate.

✓ The most important factor affecting porosity is flow rate.

✓ The two most important parameters affecting the water absorption capacity are the distance to the collector and the flow rate.

As a result, the effects of parameters (voltage, flow rate, and distance) on physical properties could not be fully explained due to extent of interaction of these terms and quadratic terms of these parameters. Different operating conditions (such as solution concentration, and collector drum rotation speed) need to be added to the experimental design in order to establish a precise control of fiber diameters and other responses. In the next study, the abovementioned parameters (solution concentration,

and drum rotation speed) will be considered to better control of fiber structures.

#### ACKNOWLEDGEMENT

The authors acknowledge the financial support of Sivas University of Science and Technology under the grant no: 2022-GENL-MUH-0008.

#### DECLARATION OF ETHICAL STANDARDS

The authors of this article declare that the materials and methods used in this study do not require ethical committee permission and/or legal-special permission.

#### CONFLICT OF INTEREST

There is no conflict of interest in this study.

#### AUTHORS' CONTRIBUTIONS

**Ebubekir Siddik AYDIN:** Conceptualization, Methodology, Investigation, Writing-original draft, Writing-review & editing.

**İbrahim KORKUT:** Methodology, Investigation, Writing-original draft, Writing-review & editing.

#### REFERENCES

- [1] Choi, D., Kil, H.S., Lee, S., "Fabrication of low-cost carbon fibers using economical precursors and advanced processing technologies", *Carbon*, 142, 610–649, (2019).
- [2] Zabihi, O., Ahmadi, M., Li, Q., Shafei, S., Huson, M.G., Naebe, M.: Carbon fibre surface modification using functionalized nanoclay, "A hierarchical interphase for fibre-reinforced polymer composites", *Composites Science and Technology*, 148, 49–58, (2017).
- [3] Atlı İ.S. and Evcin A., "Analysing mechanical behaviors of carbon fiber reinforced silicone matrix composite materials after static folding", *Journal of Polytechnic*, 23(2): 351-359, (2020).
- [4] Huang, M., Tu, H., Chen, J., Liu, R., Liang, Z., Jiang, L., Shi, X., Du, Y., Deng, H., "Chitosan-rectorite nanospheres embedded aminated polyacrylonitrile nanofibers via shoulder-to-shoulder electrospinning and electrospinning for enhanced heavy metal removal", *Applied Surface Science*, 437, 294–303, (2018).
- [5] Chauque, E.F.C., Dlamini, L.N., Adelodun, A.A., Greyling, C.J., Catherine Ngila, J., "Modification of electrospun polyacrylonitrile nanofibers with EDTA for the removal of Cd and Cr ions from water effluents", *Applied Surface Science*, 369, 19–28, (2016).
- [6] Yerkinbekova, Y., Kalybekkyzy, S., Tolganbek, N., Kahraman, M.V., Bakenov, Z., Mentbayeva, A., "Photo-crosslinked lignin/PAN electrospun separator for safe lithium-ion batteries", *Scientific Reports*, 12, 1–13, (2022).
- [7] Han, Q., Zhang, W., Han, Z., Niu, S., Zhang, J., Wang, F., Li, X., Geng, D., Yu, G., "Preparation of PAN-based carbon fiber/Co3O4 composite and potential application in structural lithium-ion battery anodes", *Ionics*, 25, 5333–5340, (2019).
- [8] Pusta, A., Tertiş, M., Cristea, C., Mirel, S., "Wearable Sensors for the Detection of Biomarkers for Wound Infection", *Biosensors*, 12, 1-12, (2021).
- [9] Khayyam, H., Jazar, R.N., Nunna, S., Golkarnarenji, G., Badii, K., Fakhrohoseini, S.M., Kumar, S., Naebe, M.,

- “PAN precursor fabrication, applications and thermal stabilization process in carbon fiber production: Experimental and mathematical modelling”, *Progress in Materials Science*, 107, 100575, (2020).
- [10] Özdemir A.O., Karataş Ç. ve Yücesu H.S., “Elyaf konfigürasyonunun termoplastik kompozit levhaların mekanik özelliklerine etkisi”, *Politeknik Dergisi*, 24(2): 599-607, (2021).
- [11] Korku M., Feyzullahoğlu E. ve İlhan R., “Farklı türlerde polyester ve çekme katkısı içeren cam elyaf takviyeli polyester kompozit malzemelerde çevresel koşulların aşınma davranışlarına olan etkilerinin incelenmesi”, *Politeknik Dergisi*, \*(\*) : \*, (\*).
- [12] Wei, Q., Xiong, F., Tan, S., Huang, L., Lan, E.H., Dunn, B., Mai, L., Wei, Q.L., Xiong, F.Y., Tan, S.S., Huang, L., Mai, L.Q., Lan, E.H., Dunn, B., “Porous One-Dimensional Nanomaterials: Design, Fabrication and Applications in Electrochemical Energy Storage”, *Advanced Materials*, 29, 1602300, (2017).
- [13] Subbiah, T., Bhat, G.S., Tock, R.W., Parameswaran, S., Ramkumar, S.S., “Electrospinning of nanofibers”, *Journal of Applied Polymer Science*, 96, 557–569, (2005).
- [14] Ali, A.A., Eltabey, M.M., Farouk, W.M., Zoalfakar, S.H., “Electrospun precursor carbon nanofibers optimization by using response surface methodology”, *Journal Electrostatics*, 72, 462–469, (2014).
- [15] Matulevicius, J., Kliucininkas, L., Martuzevicius, D., Krugly, E., Tichonovas, M., Baltrusaitis, J., “Design and characterization of electrospun polyamide nanofiber media for air filtration applications”, *Journal of Nanomaterials*, 1-13, (2014).
- [16] Campbell, F. C., “Introduction to composite materials”, *Structural composite materials*, 1, 1-29, (2010).
- [17] Andreola, F., Leonelli, C., Romagnoli, M., Miselli, P., “Techniques Used to Determine Porosity”, *American Ceramic Society Bulletin*, 79, 49–52, (2000).
- [18] Cazorla-Amorós, D., Alcaniz-Monge, J., Linares-Solano, A., “Characterization of activated carbon fibers by CO<sub>2</sub> adsorption”, *Langmuir*, 12, 2820–2824, (1996).
- [19] Jafari, M.J., Akhlaghi Pirposhteh, E., Farhangian, M., Khodakarim Ardakani, S., Tavakol, E., Dehghan, S.F., Khalilinejad, A., “Optimizing the electrospinning parameters in polyvinyl chloride nanofiber fabrication using CCD”, *Research Journal of Textile and Apparel*, 1-16, (2022).
- [20] Wei, L., Liu, C., Dong, J., Fan, X., Zhi, C., Sun, R., “Process investigation of nanofiber diameter based on linear needleless spinneret by response surface methodology”, *Polymer Testing*, 110, (2022).
- [21] Nasouri, K., Bahrambeygi, H., Rabbi, A., Shoushtari, A.M., Kafrou, A., “Modeling and optimization of electrospun PAN nanofiber diameter using response surface methodology and artificial neural networks”, *Journal of Applied Polymer Science*, 126, 127–135, (2012).
- [22] Rabbi, A., Nasouri, K., Bahrambeygi, H., Shoushtari, A.M., Babaei, M.R., “RSM and ANN Approaches for Modeling and Optimizing of Electrospun Polyurethane Nanofibers Morphology”, *Fibers and Polymers*, 13, 1007–1014, (2012).
- [23] Murphy, R., Turcott, A., Banuelos, L., Dowey, E., Goodwin, B., O’K., Cardinal, H., “SIMPoly: A Matlab-Based Image Analysis Tool to Measure Electrospun Polymer Scaffold Fiber Diameter”, *Tissue Engineering Part C: Methods*, 26(12), 628-636, (2020).
- [24] Dehghan, S.F., Golbabaie, F., Maddah, B., Latifi, M., Pezeshk, H., Hasanzadeh, M., Akbar-Khanzadeh, F., “Optimization of electrospinning parameters for polyacrylonitrile-MgO nanofibers applied in air filtration”, *Journal of the Air & Waste Management Association*, 66(9), 912-921, (2016).
- [25] Do, V.T., Nguyen-Tran, H.D., Chun, D.M., “Effect of polypropylene on the mechanical properties and water absorption of carbon-fiber-reinforced-polyamide-6/polypropylene composite”, *Composite Structures*, 150, 240–245, (2016).